

TAUVEX flight calibrations: Plans and challenges

Margarita Safonova*, P. Shalima[†] and Jayant Murthy[‡]

Indian Institute of Astrophysics, Bangalore 560034, India

Received 18 March 2009; accepted 8 May 2009

Abstract. The operational tasks for the Performance Verification (PV) and calibration phase in the first year of TAUVE X operation are presented. The new challenges regarding the possible reduction in sensitivity are outlined and are reflected in the specialized plan for first few months of the mission. The calibration operations will be extended into the first year, in parallel to an unprecedented deep exposure of the celestial poles. The preliminary zero-points of the instrumental photometric system, in AB and Vega-based magnitude systems, are calculated for pre-ground calibrations data as well as for the updated results. For flux calibration, the effective wavelengths, bandwidths and conversion factors are calculated for both pre-ground and updated values. These conversion factors are to be used for converting the TAUVE X count rates to flux and UV luminosity of the sources.

Keywords : space vehicles : instruments; instrumentation : photometers; ultra violet : general

1. Introduction

The TAUVE X (Tel-Aviv University UV Explorer) Observatory is a collaborative project between the Indian Institute of Astrophysics (IIA) and Tel Aviv University (TAU) to observe the ultraviolet (UV) sky. The Observatory will be launched as part of the GSAT-4 mission of Indian Space Research Organization (ISRO) in 2009. The major science objectives of TAUVE X are (a) searches for quasars and AGNs based on their UV properties, (b) surface photometry of galaxies in the UV, (c) studies of stars and nebulae within

*e-mail:rita@iiap.res.in

[†]e-mail:shalima@iiap.res.in

[‡]e-mail:murthy@iiap.res.in

the Galaxy, (d) the nature of the UV background, (d) properties of interstellar dust and diffuse UV background and (e) studies of UV variable sources.

The mission science goals were defined more than 15 years before the scheduled launch. During the instrument development phase these were used to form a set of requirements for calibration accuracy that guided the design of facilities and activities for the instrument ground calibration. It was realized that the change in some aspects of projected performance of the launch-ready instrument undermined some of those goals (Almoznino et al. 2009). For example, TAUVE X was expected to cover most of the UV sky during its 3-5 years of flight life. The new, restructured, mission science goals have to be considered, with the emphasis on a longer performance verification (PV) and calibrations (CAL) phase than was previously envisaged, and a reduced sky survey coverage to keep up with the required level of magnitude depth.

2. Instrument overview

2.1 TAUVE X instrument

The TAUVE X instrument is an array of three identical, 20 cm aperture, co-aligned f/8 Ritchey-Chrétian telescopes mounted on a single bezel and enclosed in a common envelope. Each telescope consists of a primary mirror, a secondary mirror, and a doublet of field-correcting lenses that maintain a relatively constant focal plane scale across the nominal field of view of 0.9° . The primary and secondary mirrors are both lightweighted zerodur, coated with Al + MgF₂. In front of each detector there is a filter wheel, with three filters and an opaque shutter, offering a total of five different UV bands for observation, and allowing simultaneous observations in two or three different wavelength bands. Field-corrector lens group, filters substrate and detector windows are all made of CaF₂, a material transparent to the UV in the range of interest of TAUVE X, and which serves as Ly- α blocker, if warmed to above $+25^\circ$ C. This is an additional measure aimed to reduce the extraneous background light (Brosch 1998).

The detectors are photon-counting imaging devices, each consisting of a proximity-focused semi-transparent CsTe photocathode, deposited on the vacuum side of the entrance window 200 μ m from the MCP surface, a stack of three microchannel plates (MCP), and a wedge-and-strip (WSZ) anode. The 25-mm active area three-stack MCP (single + chevron configuration) operate at a high-voltage gain of $\sim 10^7$, producing pulses for each incoming photon that are treated by an electronic chain, which calculates their arrival positions on the anode plate.

The instrument will be mounted on a rotating plate called the Mounting Deck Plate (MDP) on the east face of GSAT-4. Nominal operation involves scanning the sky along a fixed declination, and then change the platform orientation as required, with complete sky access archived by rotating the MDP from declination -90° to $+90^\circ$.

2.2 Instrument performance: results from ground calibrations

TAUVEX was calibrated on the ground during a six-month period in mid-2008; these data form a performance baseline for flight measurements (Almoznino et al. 2009). Resolution, background, flat field, throughput, linearity, spectral resolution and spatial distortion were measured in several sets of tests. The pre-ground calibration (pre-GC) values of effective areas were calculated on the basis of the transmissions of the telescope optics, quantum efficiencies of MCP and the geometrical area of the TAUVEX mirror assembly, given by manufacturers. During the ground calibrations (GC) the total spectral response was measured directly. The lack of MCP quantum efficiency measurements on the flight model and the deficiencies in the calibration equipment were a source of a large uncertainty in the calculation of the flight model filter transmission and, as a result, the values of the TAUVEX telescopes effective areas (A_{eff}) are uncertain to within 25%. With this uncertainty, the total spectral response was estimated as 9 times lower than expected from theoretical. The major reason for the reduction in sensitivity is suspected to be the surface contamination of the mirror assembly, though some amount of mirror degradation is not completely excluded. In addition to this, deterioration of some TAUVEX elements was detected. The following table shows suspected problems of TAUVEX structural elements.

Telescope	Detector & Filter problems	Possible cause
T2	2 defects on the detector	bad ‘pixels’
	SF1—reduced A_{eff} compared to T1-SF1 NBF3 displays damaged areas	low detector sensitivity @ $\lambda < 1750\text{\AA}$ filter structural damage
T3	SF3—reduced A_{eff} compared to T2-SF3 pinhole in SF3	low detector sensitivity @ $\lambda > 2200\text{\AA}$ filter structural damage

3. TAUVEX photometric calibration constants

It is possible that the observed reduction in photometric sensitivity is due to a reversible surface contamination of the mirrors, which may be restored during the outgassing phase right after the launch. It was therefore decided not to discard the pre-GC data and calculate photometric values for both sets. Most probably, the reality lies somewhere in between. We expect to tighten the uncertainty as the calibration is improved with flight data.

Table 1. The TAUUVEX filters and the preliminary values for the photometric calibration constants. These values will be updated once the data of the space calibration programme becomes available during the PV phase. Note the location of the filters on different telescopes.

Filter	$\Delta\lambda(\text{\AA})$			Central λ_0 (\AA)			Pivot λ_p (\AA)					
	PreGC	GC updates			PreGC	GC updates			PreGC	GC updates		
		averaged	T1	T2		T3	averaged	T1		T2	T3	averaged
SF1	506	313.7	351.6	–	1759	1739.8	1736.7	–	1755	1739	1731	–
SF2	557	517.3	–	499.8	2231	2208.0	–	2152.0	2225	2199	–	2141
SF3	616	–	595.1	687.3	2564	–	2557.6	2494.2	2556	–	2541	2472
BBF	1850	813.16	–	687.1	2496	2380.5	–	2371.1	2476	2373	–	2358
NBF3	248	–	306.8	–	2194	–	2249.8	–	2196	–	2249	–

3.1 Bandpass

The bandwidths of the filters are defined as the integrals of their normalized transmissions. We estimate the effective bandwidth of TAUVEX based on the total throughput of the system. However, we shall keep in mind that the effective bandwidth may be dependent on the spectral shape of the radiation. If most of the energy is on the falling part of the filter/system throughput curve, where the transmission is much lower than at peak, the effective bandwidths have to be calculated by integrating over wavelength the filter/system throughput curves and dividing by the throughput at the redshifted wavelengths of the lines for each source (Maoz et al. 2001). The bandwidth of a filter is

$$\Delta\lambda = \int A_{\text{norm}}(\lambda)d\lambda, \quad (1)$$

where $A_{\text{norm}}(\lambda)$ is the effective area normalized to 1. The bandwidths for TAUVEX filters for pre-ground calibration values (data averaged over all telescopes) and for the updated results from the ground calibrations are presented in Table 1.

3.2 Pivot wavelength

A source-independent relationship between AB and STmag magnitude systems (see Sec. 3.5 below) can be determined at the so-called *pivot* wavelength λ_p ,

$$\lambda_p^2 = \frac{\int A(\lambda)\lambda d\lambda}{\int A(\lambda)d\lambda/\lambda} \quad (2)$$

where $A(\lambda)$ is TAUVEX effective areas. The pivot wavelengths for TAUVEX filters are presented in Table 1.

3.3 Central (or mean) wavelength

The central (or mean) wavelength of a filter, by a general definition (Budding & Demircan 2007), is equal to

$$\lambda_0 = \frac{\int \lambda T(\lambda)d\lambda}{\int T(\lambda)d\lambda}, \quad (3)$$

where $T(\lambda)$ is the normalized transmission of a filter as a function of wavelength. We assume for TAUVEX the normalized effective area curves instead of pure transmission curves. Thus, the central (or mean) wavelengths of TAUVEX filters are given by

$$\lambda_0 = \frac{\int \lambda A(\lambda)d\lambda}{\int A(\lambda)d\lambda}, \quad (4)$$

where $A(\lambda)$ is the effective areas normalized to 1. Table 1 displays the central wavelengths for TAUVEX filters.

However, while λ_0 does not depend on the spectrum of the source, it is precisely representative only where the filter bandwidth is negligible in comparison to that. The effect of the source power distribution over a given broadband filter is included in its effective wavelength λ_{eff} (Sec. 3.4).

3.4 Effective wavelength

Effective wavelength for TAUVE X filters is defined as

$$\lambda_{\text{eff}} = \frac{\int \lambda A(\lambda) F(\lambda) d\lambda}{\int A(\lambda) F(\lambda) d\lambda}, \quad (5)$$

where $F(\lambda)$ is the source spectrum in $\text{ergs/cm}^2/\text{sec}/\text{\AA}$. This is the mean wavelength of the passband as weighted by the energy distribution of the source over the band. In Tables 2 and 4 the effective wavelengths for objects of several basic spectral types and few representative galaxies are presented for both pre-ground calibration values and the updated ones. Stellar spectra were obtained from TAUVE X online flux calculator, white dwarfs spectra were obtained from the CALSPEC database and galaxies template spectra from STScI Calibration Database System (<ftp://ftp.stsci.edu/cdbs/grid/kc96>).

3.5 UV flux calculations and zero-points

Real flux in physical units (for eg., in $\text{erg/cm}^2/\text{sec}/\text{\AA}$) allows direct comparison with models and also with measurements made with different instruments. That is why we have made an attempt to define a direct conversion from measured counts to flux received from the source. It can be done by following any of the methods we outline below, either by using the counts-to-flux conversion factors, or the magnitude systems. Since in the UV there is no universally standard photometric system, we have implemented several different magnitude systems that will allow the users to compare their data with other instruments, and have calculated photometric zero-points for these systems. The zero-points set the brightness scale of the instrument system in a given bandpass. By definition, it is the magnitude of an object that would generate a count rate of 1 count/sec in the specified observational configuration (i.e. combination of detector and filter). The setting of the zero-point determines the connection between observed counts and a standard photometric system and, in turn, between counts and astrophysically interesting measurements such as the flux incident on the telescope.

Spectral Type Dependent Flux Conversion: The count-to-flux conversion factors are a function of the intrinsic source spectrum. The flux of the observed object can be obtained by multiplying the observed count rate by the, most appropriate for the chosen

Table 2. The TAUVE X filters and the pre-flight values for the effective wavelengths. These values will be updated once the data of the space calibration programme becomes available after the PV phase. Note the location of the filters on different telescopes.

Filter	Effective Wavelength λ_{eff} (Å)											
	Vega			O0V star			B0V star					
	PreGC	T1	T2	T3	PreGC	T1	T2	T3	PreGC	T1	T2	T3
SF1	1768	1746.0	1744.2	—	1709	1706.3	1681.2	—	1718	1713.0	1689.0	—
SF2	2205	2179.5	—	2128.3	2168	2116.1	—	2045.0	2179	2134.7	—	2067.0
SF3	2553	—	2534.8	2459.2	2472	—	2384.8	2288.2	2484	—	2415.4	2323.6
BBF	2495	2393.3	—	2348.9	2342	2287.2	—	2258.8	2359	2301.1	—	2273.0
NBF3	2187	—	2238.0	—	2183	—	2217.1	—	2187	—	2223.8	—
Filter	A0V star			F0V star			G0V star					
	PreGC	T1	T2	T3	PreGC	T1	T2	T3	PreGC	T1	T2	T3
	SF1	1768	1746.0	1744.2	—	1936	1896.7	1972.4	—	2051	2211.3	2460.6
SF2	2205	2179.6	—	2128.3	2290	2282.0	—	2237.1	2444	2410.8	—	2366.7
SF3	2553	—	2534.8	2128.3	2646	—	2671.7	2636.7	2726	—	2755.8	2745.2
BBF	2495	2393.3	—	2349.0	2713	2564.5	—	2516.6	2952	2794.3	—	2734.8
NBF3	2187	—	2238.0	—	2196	—	2270.0	—	2219	—	2334.9	—
Filter	G191B2B white dwarf			GD71 white dwarf								
	PreGC	T1	T2	T3	PreGC	T1	T2	T3				
	SF1	1701.6	1702.0	1675.0	—	1703.7	1677.6	—				
SF2	2165.9	2112.7	—	2037.9	2167.2	—	2040.7					
SF3	2470.4	—	2379.1	—	2473.3	—	—					
BBF	2341.2	2288.9	—	2258.6	2344.9	—	—					
NBF3	2181.5	—	2215.0	—	2182.8	—	—					

Table 3. Conversion factors after the ground calibrations. These values will be updated once the data of the space calibration programme becomes available after the PV phase. Due to the space constraints we have not presented the pre-GC values, they are available on the TAUVEEX webpage.

Tel.	Filter	Conversion factor (erg/cm ² /Å/cnt)								
		O0V	B0V	A0V	F0V	G0V	GD71	G191B2B		
Telesc. 1	SF1	2.63×10^{-13}	2.6×10^{-13}	2.57×10^{-13}	2.36×10^{-13}	2.03×10^{-13}	2.63×10^{-13}	2.64×10^{-13}		
	SF2	3.98×10^{-14}	3.94×10^{-14}	3.86×10^{-14}	3.69×10^{-14}	3.49×10^{-14}	3.98×10^{-14}	3.99×10^{-14}		
	BBF	1.06×10^{-14}	1.06×10^{-14}	1.02×10^{-14}	9.63×10^{-15}	8.99×10^{-15}	1.06×10^{-14}	1.06×10^{-14}		
Telesc. 2	SF1	4.3×10^{-13}	4.28×10^{-13}	4.14×10^{-13}	3.67×10^{-13}	2.94×10^{-13}	4.31×10^{-13}	4.32×10^{-13}		
	SF3	5.53×10^{-14}	5.46×10^{-14}	5.2×10^{-14}	4.94×10^{-14}	4.79×10^{-14}	5.53×10^{-14}	5.54×10^{-14}		
	NBF3	1.97×10^{-13}	1.98×10^{-13}	1.96×10^{-13}	1.94×10^{-13}	1.89×10^{-13}	1.97×10^{-13}	1.99×10^{-13}		
Telesc. 3	SF2	4.13×10^{-14}	4.09×10^{-14}	3.97×10^{-14}	3.78×10^{-14}	3.57×10^{-14}	4.14×10^{-14}	4.15×10^{-14}		
	SF3	8.04×10^{-14}	7.92×10^{-14}	7.48×10^{-14}	6.98×10^{-14}	6.7×10^{-14}	8.05×10^{-14}	8.07×10^{-14}		
	BBF	1.28×10^{-14}	1.27×10^{-14}	1.23×10^{-14}	1.15×10^{-14}	1.07×10^{-14}	1.28×10^{-14}	1.28×10^{-14}		

Table 4. Effective wavelengths and count-to-flux conversion factors for few representative galaxies template spectra. The templates are obtained from the Kinney-Calzetti Spectral Atlas of Galaxies.[†]

Tel.	Filter	Effective wavelength λ_{eff} (Å)			Conversion factor (erg/cm ² /Å/cnt)		
		Elliptical	Sa spiral	Starburst [‡]	Elliptical	Sa Spiral	Starburst [†]
Telesc. 1	SF1	1737.9	1751.3	1723.5	2.583×10^{-13}	2.564×10^{-13}	2.604×10^{-13}
	SF2	2200.8	2234.7	2164.3	3.825×10^{-14}	3.767×10^{-14}	3.89×10^{-14}
	BBF	2456.8	2493.6	2343.6	9.895×10^{-15}	9.573×10^{-15}	1.037×10^{-14}
Telesc. 2	SF1	1735.3	1756.3	1707.9	4.168×10^{-13}	4.118×10^{-13}	4.234×10^{-13}
	SF3	2609.9	2631.7	2481.9	5.054×10^{-14}	5.012×10^{-14}	5.315×10^{-14}
	NBF3	2239.3	2263.0	2235.3	1.966×10^{-13}	1.946×10^{-13}	1.970×10^{-13}
Telesc. 3	SF2	2149.7	2177.0	2103.4	3.933×10^{-14}	3.883×10^{-14}	4.019×10^{-14}
	SF3	2536.8	2578.6	2399.0	7.255×10^{-14}	7.137×10^{-14}	7.672×10^{-14}
	BBF	2427.2	2470.9	2314.8	1.192×10^{-14}	1.171×10^{-14}	1.250×10^{-14}

[†] Calibration Database System, Space Science Telescope Institute's ftp site: <ftp://ftp.stsci.edu/cdbs/grid/kc96>

[‡] This template is for low ($E(B - V) < 0.10$) internal extinction starburst galaxy.

Table 5. Preliminary values for Vega zeropoints.

Filter	Zero-point _{Vega}			
	Pre-ground calibrations	Ground calibrations updates		
	averaged values	T1	T2	T3
SF1	13.6	10.84	10.84	–
SF2	14.78	12.68	–	12.68
SF3	14.45	–	12.2	11.85
BBF	16.45	14.06	–	13.86
NBF3	13.58	–	10.86	–

spectral type and filter, conversion factor, selected from Tables 3 and 4. The numbers in Tables 3 and 4 have been obtained by convolving the spectra of stars, obtained from the TAUVE X online flux calculator, or template galaxies SEDs, respectively, with the GC-updated effective areas of the filters, and dividing the resulting in-band fluxes by the expected count rate, obtained from the TAUVE X online Exposure Time Calculator (ETC). In Table 3 we also present the average conversion factors for two standard white dwarfs. They give an average transformation which can be used in all cases when no information is available on the spectral characteristics of the source. A calibration observing campaign will be carried out in order to obtain the most reliable conversion factors for each stellar type. Conversion factors can be used to calculate the average stellar UV luminosity,

$$L_{UV} = 4\pi d_*^2 \cdot G \cdot \Delta\lambda \cdot CPS_{Filter} , \quad (6)$$

where d_* is the distance to the source, G is the conversion factor, $\Delta\lambda$ is the bandwidth of the filter and CPS_{Filter} is the count rate in that filter.

General method. Flux based on Vega flux scale: The standard and reference for all classical broad-band photometry is the magnitude system based on Vega flux. The instrumental magnitude has to be calculated using the formula

$$m = -2.5 \log_{10}(CPS) + \text{Zero-point}_{Vega} , \quad (7)$$

where Vega zero-points have been derived for TAUVE X for each filter by using the equation

$$\text{Zero-point}_{Vega} = 2.5 \log_{10}(CPS_{Vega}) + m_{Vega} . \quad (8)$$

Vega zero-points have been defined in such a way that Vega has $m_{Vega} = 0.025$ in all TAUVE X filters (following the convention of XMM-Newton, see for e.g., Stuhlinger et al. 2007).

The popular flux-based systems at UV and visible wavelengths are the monochromatic AB and STmag (Space telescope magnitude) systems. Both define an equivalent flux density for a source, corresponding to the flux density of a source of a predefined spectral shape that would produce the observed count rate, and convert this equivalent flux to a magnitude. The conversion is chosen so that the magnitude in V corresponds roughly to that in the Johnson system. AB and STmag zero-points for TAUVE X are presented in Table 6.

AB magnitude system: In AB system, the flux density is expressed per unit frequency and the reference spectrum is flat in F_ν . AB system is defined as

$$m_{\text{AB}}^{\text{Filter}} = \text{Zero-point}_{\text{AB}}^{\text{Filter}} - 2.5 \log_{10}(\text{CPS}^{\text{Filter}}), \quad (9)$$

where the zero-points for each filter come from the original definition of AB magnitude as

$$\text{Zero-point}_{\text{AB}}^{\text{Filter}} = -48.60 - 2.5 \log_{10}(1/n_{\text{phot}}), \quad (10)$$

with n_{phot} being the count rate measured in a filter for a constant incoming flux $f_\nu = 1 \text{ erg/sec/cm}^2/\text{Hz}$. A great advantage of AB magnitudes is that the conversion to physical units can be easily obtained,

$$F_\nu = 3631 \times 10^{-0.4m_{\text{AB}}} \text{ (Jy)}. \quad (11)$$

Table 6. TAUVE X filters and the preliminary values for AB and STmag zero-points.

Filter	Zero-point _{AB}				Zero-point _{ST}			
	Pre-GC	GC updates			Pre-GC	GC updates		
	averaged values	T1	T2	T3	averaged values	T1	T2	T3
SF1	15.75	12.9	12.4	–	13.24	10.4	9.9	–
SF2	16.67	14.49	–	14.5	14.65	12.5	–	12.5
SF3	16.2	–	13.84	13.52	14.48	–	12.2	11.8
BBF	18.2	15.75	–	15.57	16.42	13.9	–	13.7
NBF3	15.4	–	12.66	–	13.43	–	10.7	–

ST magnitude system: STmag system is based on a spectrum with constant flux density per unit wavelength f_λ and an approximate Vega zero-point. Another way to express this zero-point is to say that an object with $f_\lambda = 3.63 \times 10^{-9} \text{ erg/sec/cm}^2/\text{\AA}$ will

have magnitude STmag=0 in every filter. This is the flux of Vega at 5500 Å; hence a star of Vega's brightness at 5500 Å is defined to have $m = 0$. The instrumental magnitude is

$$m_{\text{ST}}^{\text{Filter}} = \text{Zero-point}_{\text{ST}}^{\text{Filter}} - 2.5 \log_{10}(CPS^{\text{Filter}}). \quad (12)$$

STmag system is related to AB system through a source-independent relation at a pivot wavelength (see Sec. 3.2),

$$F_{\lambda} = F_{\nu} \cdot \frac{c}{\lambda_p^2 \cdot 10^8}, \quad (13)$$

where the factor 10^8 comes from the conversion of cm to Å. The STmag zero-points thus will be

$$\text{Zero-point}_{\text{ST}}^{\text{Filter}} = \text{Zero-point}_{\text{AB}}^{\text{Filter}} + 5 \log \lambda_p - 18.7. \quad (14)$$

4. Space calibration programme

The primary goal of TAUVE X in-flight calibration programme is to ensure that the obtained set of images and maps can be used for the astronomical data analysis to the level required for scientific investigations. The calibration activities can be broadly divided into the following list of calibrations.

4.1 Pre-survey observations

Before commencing calibration operations numerous checks are required to verify the health and safety of the Observatory and to determine the best modes of operation. The Outgassing mode will be initiated immediately following the deployment of the solar panels and TAUVE X will be kept in this mode (heated) for at least 25 days to allow sufficient time for any contaminants carried up with the satellite to outgas and disperse so that they would not freeze on the cold optics.

Two weeks later, we will test the telemetry reception, verify the scientific data channel, test the pipeline and obtain the images of the BIT calibration lamps. Synthetic events will be transmitted to the input of the analog-front-end (AFE) cards and treated there as real events. This will be used to measure the DC offset of the W, S, and Z values coming out of the detector pre-amplifier. The BIT lamps are the internal calibration source, and will be used to verify the functioning of the detectors and filters and to track changes in their sensitivity while in orbit. The BIT lamps flight images will also be compared with ground calibrations images and with known standard stars in the sky.

This period will be followed by a PV and calibration phase for about 65 days. This phase will include a period of repeated surveying on a limited region of sky to verify the survey strategy and the data processing facilities. The scans of this "minisurvey" will be hand-tailored for maximum efficiency in coverage. After all these tests have been completed and the problems if any resolved, the Northern Galactic Plane survey (NOGAPS) will start (if the launch proceeds as scheduled, in mid-2009).

4.2 Photometric accuracy

The usefulness of TAUVEX image database is determined by the ability to provide reliable way of reconstructing the fluxes of astronomical targets. Thus, an absolute photometric accuracy is the ability to determine the true flux of a source. This flux can be determined as a bandpass-averaged flux within the instrument band. Zero-point accuracy denotes errors in the conversion between a measured count rate and a band-averaged instrumental flux. Band-shape accuracy relates to errors in the conversion between a band-averaged instrumental flux and the apparent magnitude of a source with a given SED.

The best way to calibrate TAUVEX photometry will be to perform repeated observations of carefully selected celestial sources. We will measure the broad-band flux of spectrophotometric standards and calculate the first-order zero-points. Comparing it with the pre-flight zero-points, we will define the zero-point corrections. We have compiled the list of the calibration standards in Table 7. TAUVEX primary standards are mostly HST white dwarf stars that have been chosen from the wide range (at least 5 magnitudes) in UV intensity, and for which UV and optical spectra on the white dwarf scale are available. Stars in Table 7 are assigned different priorities, priority 1 being the ones that are at high southern latitudes as, due to the seasonal constraints, the beginning of the mission TAUVEX will mostly spend in the region of South ecliptic Pole. Priority 2 assigned to the stars at lower southern latitudes which means reduced exposure time for TAUVEX and increased number of scans. Stars with priority 3 form the complementary sets needed to extend the sky coverage and they will be observed in the course of normal survey observations. The calculated count rates and magnitudes for the three magnitude systems for these standards are put up on the TAUVEX website (<http://tauvex.iap.res.in>). In Table 8 we present, as an example, the expected AB magnitudes for each filter and telescope for the two standard white dwarfs, and Table 9 shows a comparison of the AB magnitudes obtained with TAUVEX, GALEX and XMM-Newton optical monitor (XMM_OM). We should note that the bandpasses of TAUVEX filters are not exactly the same as those of GALEX and XMM_OM.

4.3 Astrometric calibrations

4.3.1 Boresight and alignment

The telescopes have been aligned to an accuracy of $1'-2'$ as part of the mechanical integration process already completed at ElOp and have been locked into place. Once at the ISAC integration facility, the telescope structure will be aligned to the MDP using an optical flat to a precision of within $6'$. However, it is possible that some flexing of the telescope structure may occur during launch and we will test the overall alignment

Table 7. A sample of TAUVE X photometric calibration targets.

Identifier	α	δ	Sp. Type	m_V	HST std	IUE [†]	Model	Priority
BPM16274	00:50:03.51	-52:08:15.70	DA2	14.2	+	+	+	1
HD60753	07:33:27.32	-50:35:03.32	B3IV	6.7	+	+	+	1
HD49798	06:48:04.70	-44:18:58.43	O6	8.3	+	+	+	2
HR1996	05:45:59.89	-32:18:23.17	O9V	5.17	+	+	+	2
NGC7293	22:29:38.55	-20:50:13.60	V. Hot	13.53	+	+	+	2
LTT9491	23:19:35.44	-17:05:28.40	DC	14.1		+	+	3
L119-34	22:19:48.48	-65:29:18.40	DZ5	14.43		+		3
RE J2009-605	20:09:05.24	-60:25:41.60	DA1	13.4		+		3
MCT2000-5611	20:04:18.10	-56:02:46.00	DA	15.2		+		3
L210-114	20:18:54.90	-57:21:34.00	DA2	13.73		+		3

Column (1): Standard identifier; columns (2)&(3): J2000 coordinates (α is in (hh:mm:ss) and δ is in (dd:mm:ss) format, respectively); column (4): spectral type of the object; column (5): apparent V magnitude; column (6) indicates whether a star is an HST standard; column (7) indicates whether an IUE spectra is available; column (8) indicates whether a model spectra (CALSPEC database) is available; column (9) assigns the priority (explanations in the text).

[†] Holberg et al. 2003.

Table 8. TAUVE X AB magnitudes for HST standards.

Filter	AB magnitudes					
	GD71 [†] ($U = 11.676$)			G191B2B [†] ($U = 10.24$)		
	T1	T2	T3	T1	T2	T3
BBF	11.83	–	11.81	10.32	–	10.30
SF1	11.37	11.36	–	9.86	9.85	–
SF2	11.71	–	11.65	10.20	–	10.14
SF3	–	11.89	11.86	–	10.41	10.37
NBF3	–	11.76	–	–	10.25	–

[†] U magnitudes are from Horberg & Bergeron 2006.

Table 9. Comparison of magnitudes in AB system for two reference sources.

Star	TAU filter ($\lambda_{\text{eff}}^{\dagger}$, Å)	AB_TAU	XMM filter (λ_{eff} , Å)	AB_XMM ^{††}	AB_GALEX (2271 Å)
BD+332642 Sp.Type B2IV	T3-SF2 (2134)	10.5122	UVW2 (2120)	10.4329	10.47
	T3-BBF (2303)	10.5237	UVM2 (2310)	10.4522	
	T2-SF3 (2415)	10.5284	UVW1 (2910)	10.3756	
G93-48 Sp.Type DA3	T1-SF2 (2114)	12.4112	UVW2 (2120)	12.3650	12.39
	T1-BBF (2290)	12.4689	UVM2 (2310)	12.3820	
	T2-SF3 (2384)	12.5120	UVW1 (2910)	12.5384	

[†] effective wavelengths for TAUVE X filters are from Table 2 in this paper for a given spectral type.

^{††} XMM.OM and GALEX data are from Stuhlinger et al. 2007.

in orbit. Selected fields will be observed with the specific goal of deriving an astrometric correction. We have scheduled a number of bright fields in the PV phase (Table 10), mainly open clusters that contain many stars.

Some part of this calibration task will be fulfilled by the daily operations of the mission. TAUVE X is a scanning instrument with a large field of view which will observe many stars while scanning over the sky. The apparent position of these objects will be compared with the true position to derive an astrometric correction over the entire field of view.

4.3.2 Distortion correction

The pipeline includes two corrections for the spatial positions of the stars in the field. The first is an alignment matrix to align the boresights of the three telescopes. In principle,

this should be an identity matrix but can account for both translation and rotation of the telescope structure with respect to each other and to the MDP. The second is a distortion correction which corrects for the internal distortion in each telescope, almost entirely due to electrostatic fields in the detector. We have implemented a distortion correction consisting of a sixth order polynomial in x and y which converts the detector coordinates to an orthogonal grid.

Table 10. Open clusters for astrometric calibration.

Identifier	α	δ	Dim _V (')	Distance (pc)	No. of stars
Mamajek 1	08:42:06	-79:01:38	40	97	18
Feigelson 1	11:59:51	-78:12:27	18	114	10
ASCC 51	09:18:00	-69:41:24	48	650	18
NGC 1901	05:18:11	-68:27:00	10	460	16
ASCC 76	13:52:16	-66:24:00	42	600	11
BH 164	14:48:14	-66:20:12	60	541	14

Column (1): Standard identifier; columns (2)&(3): J2000 coordinates (α is in (hh:mm:ss) and δ is in (dd:mm:ss) format, respectively); column (4): cluster size in V-band in arcmins; column (5): distance from the Sun in parsecs; column (6): number of stars in a cluster.

4.3.3 Correction for spacecraft motion

In addition to the scanning motion of TAUVE X, we will have to correct for the spacecraft motion during an observation. The spacecraft will move as a function of time and this motion will have a power spectrum. The long timescale variations are drift and the high frequency variations are jitter. While the drift may be high, 180 arcsec for 200 seconds (normally by the ISRO specifications), the jitter (which is defined to have a frequency of > 0.1 Hz) is very small in terms of TAUVE X resolution. The TAUVE X data pipeline automatically corrects for all spacecraft motion by registering the positions of the stars in each frame and shifting the frames so that the positions match. This is a robust method that has been used in other missions and we anticipate no difficulty in applying it to TAUVE X.

We are now implementing procedures to derive all astrometric corrections from the PV phase data. The actual derivation of the corrections is done by the TAUVE X team and is fed back into the pipeline. A regular program of checking the astrometric corrections is planned and parameters and corrections will be updated as the mission progresses.

4.4 Coincidence loss (Linearity)

Non-linearity in the detected counts can be either due to a bright point source or due to high straylight in the FOV. Non-linearity at high event rates is caused by rejection of

events that come less than Δt within each other (in such a case both events are rejected). The detectors have a response time of 200 ns, which leads to two events as a single event if they occur within 200 ns of each other but not to the rejection of event. The dead-time that defines the performance of the signal processing electronics at high input rates is the dead-time Δt of one signal processing by an Analog-Front-End (AFE) card of TAUVEX, and it is $\Delta t \sim 3 \mu\text{sec}$ (Safonova 2008; Almoznino et al. 2009). Thus, the number of events actually registered is limited by the AFE cards. However, since Δt is not known accurately, the approach is to use the trigger data, which is linear to the actual rate up to $\sim 2.0 \times 10^5$ counts/sec. A measurement of the ratio between the trigger rate and the event rate at low event rates (where the event rate is linear) gives the basis for the correction of the event rate at high photon rates. The algorithm for the correction is described in (Almoznino et al. 2009). The best way is to correct whenever the event rate exceeds the linear regime.

Case 1. High total count rate: In the case of the non-linearity being the result of the entire field being bright, ground measurements can be used to obtain a function which will give the actual count rate from the observed count rate.

Case 2. Bright point source: In the case of bright point sources being responsible for the non-linearity, this can be measured by observing stars of known magnitudes and then used to predict the actual fluxes of observed sources. This will be done only after correcting for the non-linearity in the total count rate (Case 1). The count rate should also be corrected for dead time using the frame-time and the dead-time fraction.

We will observe stars with a wide range of magnitudes in order to get a curve for the value of the coincidence loss. The calibration stars given in Table 7 will be used for this test.

4.5 Point Spread Function (PSF) fitting

During the ground calibrations, the PSF was measured across the detector plane using an array of 25 pinholes and a xenon lamp as the source (Almoznino et al. 2009). Fig. 1 shows a 3-D graph of the PSF (corresponding to an image of one of the pinholes) observed by telescope T3 with the SF3 filter. The average FWHM measured for this telescope-filter combination is 106.3 ± 15.9 microns.

In space, the PSF is generally determined by observing a star field, such as an open cluster. Although TAUVEX is a scanning instrument, the PSF can be measured since the scanning smear is smaller than 1/3 of the expected PSF (14 arcsec) in every 0.128 sec sub-frame. In addition, the pixel size is much bigger for the TAUVEX detectors compared to optical detectors, resulting in an under-sampled PSF which, as such, should

not vary much over the field of view. In the case of TAUVEEX, a point source would make an image with a FWHM of ~ 4 pixels, that would contain 30% of the energy (TAUVEEX plate-scale is equal to 3.538 arcsec/pixel (Almozino et al. 2009)). To collect 90% of the energy we would have to go to an aperture of ~ 9 pixels. We will characterize the PSF using observations of stars passing through the field of view during normal operations. In addition, we will also use the field oriented calibration observations such as those of clusters for the flat field and distortion. The PSF fitting is not used in the normal operation of the pipeline but will be necessary for accurate photometry and separation of sources in crowded fields.

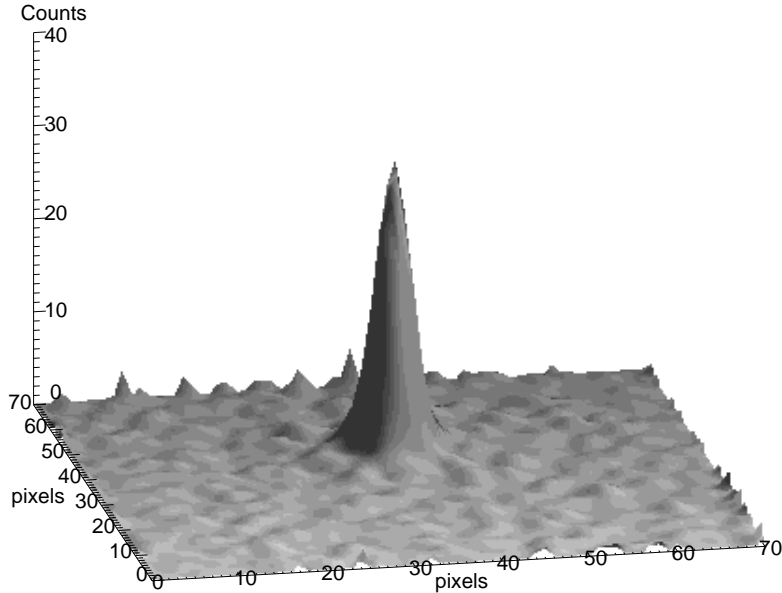


Figure 1. PSF measured during the ground calibration on telescope T3 with the SF3 filter. The z-axis shows the total counts observed during the entire exposure.

4.6 Largescale sensitivity (Flat field)

The flat field is a map of the relative pixel-to-pixel variations over the detector and generally requires accurate photometry of stars over the entire field. A one-dimensional subset is possible without accurate photometry because all stars are scanned across lines of equal declination, and repeated scans with small offsets of a set of sources will allow a flat fielding of the entire detector, at the cost of several days of observations. The open clusters given in Table 10 will be used for the purpose. It should be noted that the sensitivity of this, as with many of the calibrations, will be limited by intrinsic photon

noise, whereas the ground calibration observations had a much better accuracy of at least 1.5 % per resolution element (Almozino et al. 2009). Therefore the on-orbit measurements will be used to check the consistency of the ground measurements.

4.7 Red leak

Many UV instruments have a red leak (long-wavelength transmission) which can lead to contamination from cool stars in the field. This can be tested by observing stars which do not emit in the UV, such as M-type stars. Any counts detected in the UV give a measure of the red leak. Table 11 gives the list of candidate stars (we have calculated the expected counts, though we did not include them here due to the space constraints). Solar light scattering can also be used as a good test for red leak measurement. This will be done as part of routine observations.

Table 11. Candidate stars for determining the red leak.

Name	α	δ	m_V
HD66342	119.9064	-60.5871	5.17
HD97778	168.8010	23.0955	4.63
HD108903	187.7915	-57.1132	1.63
HD120323	207.3613	-34.4508	4.19
HD122250	211.3328	-76.7968	5.5
HD145366	245.0867	-78.6957	4.68
HD156014	258.662	14.3903	3.48
LHS449	262.1664	-46.8952	9.36
LHS3685	323.3916	-49.0090	8.67

Column (1): Star name; columns (2)-(3): J2000 coordinates (in degrees); column (4): V-band magnitude.

4.8 Light leak test

Even through the opaque shutter some photons may still manage to reach the detector. This is known as a light leak. If present, this will be measured by “closing the filters” (turning all filter wheels to the opaque shutter) - any photons detected would give the amount of light leak. This test is scheduled in the very beginning of the PV phase, during the first three orbits.

4.9 Straylight rejection

Solar light: One of the possible sources of stray light would be the sunlight scattered off the spacecraft surfaces. This may be a complex function of the solar angle and the look direction. We have developed a model for the scattered light, described in *Observational Windows and Limiting Magnitude Maps* document (<http://tauvex.iiap.res.in>), but this was based on an incomplete understanding of the reflective and scattering properties of the spacecraft surfaces.

The scattering of sunlight from the spacecraft surfaces is one among a number of sources which contribute to the diffuse background in a typical image. These ranges from instrumental sources to airglow, zodiacal light and the astrophysical signal (see Murthy (2009) for a recent review) and cannot be easily distinguished with an imaging instrument. However, we can observe at different solar angles when only the level of solar scattering is different and infer the different contributions.

Bright point and extended sources: Due to the scanning nature of the TAUVE X instrument, many bright sources will be observed or will be close to the field of view. We currently adhere to a bright star constraint of 20,000 counts/sec over the whole detector. This significant constraint is being enforced in the early stage of the mission to avoid affecting the MCP gain. While some sources may force us to shutdown the instrument or close the filters, it is nevertheless useful to measure the straylight from objects which are out of, but near to, the field of view of TAUVE X. Although this has been done on the ground, the space-based measurements are much more reliable and therefore will be done during the first few months after the launch.

Some part of this test may be done serendipitously as TAUVE X scans the sky, however, special tests will also be scheduled. This test may have to be done in several stages with progressively closer observations to bright stars, or even the Moon, due to safety considerations.

5. Conclusions

Overall, the flight calibration campaign does not have the sound under-pinning of a successful ground calibration programme that has been anticipated. As with all space missions, the actual calibration of TAUVE X will come from its performance in space. We have drawn up a mission plan which will characterize the instrument performance under a wide variety of conditions. This is particularly important in the case of TAUVE X because of the difficulties encountered during the ground calibration of the instrument. The TAUVE X calibration is also complicated by the operating mode of the spacecraft in that the longest exposures will be in the Polar regions.

In order to address all these issues, we have devoted the first three months of the mission (after about 3 weeks of outgassing) to the instrument characterization. Assuming a launch in mid-2009, as planned, we will observe sources in the Southern hemisphere, particularly fields near the South Pole, where we will get exposure times of greater than 10,000 seconds per day. We have chosen a mix of primary and secondary standards for photometric calibrations and have chosen crowded fields to test the distortion, flat fielding and other global properties of the instrument. We will also continue building up the calibration knowledge during the course of normal survey observations so that science data and calibration will go hand in hand. Most of the efforts of our calibration programme thus will have to rely on celestial targets, not necessarily the primary standards.

We expect that we will emerge with a well-characterized instrument which will yield outstanding scientific results on a number of astrophysical problems. Updates to the status of the instrument and the latest calibration results may always be obtained from the main TAUVE X web site at <http://tauvex.iap.res.in>.

Acknowledgments

Authors would like to thank members of the TAUVE X Core Team, Noah Brosch and Elhanan Almozino, for many fruitful discussions during the writing of this paper. We are also thankful to the anonymous referee for insightful comments.

References

- Almozino, E. et al., 2009, *Ap&SS*, 320, 321
- Brosch, N., 1998, *PhyS*, T77, 16
- Budding, E., & Demircan, O., 2007, in *Introduction to Astronomical Photometry, 2007*, 2nd edition, Cambridge: Cambridge University Press
- Holberg, J. B., Barstow, M. A., Burleigh, M. R., 2003, *ApJS*, 147, 145
- Holberg, J. B., P. Bergeron, 2006, *ApJ*, 132, 1221
- Maoz, D., et al., 2001, *AJ*, 121, 3048
- Murthy, J., 2009, *Astrophys. Space Sci.*, 320, 21
- Safonova, M., TAUVE X Detectors and Brightness Protection, 2008, TAUVE X Core Team Publication, <http://tauvex.iap.res.in>
- Stuhlinger, M., et al., 2007, XMM-SOC-CAL-TN-0052 Issue 4.0, XMM-Newton Science Operation Centre